Perjanjian No: III/LPPM/2013-03/02-P

ULTRASONIC-ASSISTED DRYING AND INTERMITTENT DRYING: A MODELING STUDY USING THE REACTION ENGINEERING APPROACH (REA)

Disusun Oleh:
Aditya Putranto, S.T., M.T., M.Sc., Ph.D.

Lembaga Penelitian dan Pengabdian kepada Masyarakat
Universitas Katolik Parahyangan
2013

ABSTRACT

Drying is a simultaneous heat and mass transfer process which involves significant energy consumption. For sustainable processing practice, ultrasonic-assisted drying is often implemented. In order to assist in process design and optimization, a physically-meaningful drying model is useful. The REA (reaction engineering approach), which has been shown to be accurate to model several challenging drying cases, is implemented here to model the ultrasonic-assisted drying with various intensities. The relative activation energy ($\Delta E_{v,b}$) generated from one accurate drying experiment is used to model the ultrasound-assisted drying with various intensities. The results of modeling match very well with the experimental data. The REA is accurate to model the ultrasonic-assisted drying. The mechanisms of ultrasonic-assisted drying can be explained well by the REA. A landmark for process intensification of drying process has been set up by the REA. The model can be readily adopted in industrial settings for process design and optimization.

CHAPTER 1

INTRODUCTION

1.1. Background

Drying is a process of water removal involving simultaneous heat and mass transfer process. Study of drying is important since drying is an energy-intensive process and affects the product quality. Several drying schemes, controlled drying operations and process intensification of drying need to be implemented to minimize energy consumption of drying and maintain the product quality of the materials being dried (Chou at al, 2000; Chua et al, 2001; Allanic et al, 2006; Shi et al, 2008; Garcia-Perez et al, 2007). Innovative process design of dryer and exploration of operating conditions of dryer were also conducted in order to reduce the energy consumption and maintain the product quality (Huang et al, 2003; 2004; Wu et al, 2007; Woo et al, 2008; Jin and Chen, 2009[a,b]; Jamalladine and Ray, 2010).

Drying was reported to require significantly large amount of energy since it requires large heat for evaporating water (Midili et al, 2001; 2002; Dincer, 2002[a,b]). However, not all the heat supplied is received by the product being dried since there is usually heat carried by hot air vent, flue gas loss, convection loss, loss to ground as well as loss to structure (Tippayawong et al, 2008). The energy consumption was reported to be very dependent on the drying methods and operating conditions (Sharma and Prasad, 2006; Koyuncu et al, 2007; Motevali et al, 2011[a,b]). Microwave drying was shown to give the least specific energy consumption followed by the combined hot air and infrared heating drying while the convective drying alone resulted in the highest specific energy consumption (Motevali et al, 2011[b]). For convective drying, the decrease of velocity and increase of temperature decreased the specific energy consumption while for infrared heating drying, the increase of infrared-heating intensity decreased the specific energy consumption (Sharma and Prasad, 2006; Koyuncu et al, 2007; Motevali et al, 2011[a,b]).

Drying was shown to affect the product quality of the materials being dried significantly. For food materials, drying was shown to influence the loss of ascorbic acid, volatiles, aroma and caretenoids (Timoumi et al, 2007; Di Scala and Crapiste, 2008; Mrad et

al, 2012; Ramallo and Mascheroni, 2012). Degradation of ascorbic and caretenoids was shown to be more enhanced with the increase of drying air temperature and product moisture content (Di Scala and Crapiste, 2008). The rehydration ability and ascorbic acid retention were dependent on the drying air temperature (Ramallo and Mascheroni, 2012). Similarly, the increase of temperature enhanced the loss of aroma (Timoumi et al, 2007). The survival of probiotics was also found to be very dependent on the temperature and moisture content (Huang et al, 2009). Drying was shown to induce fissuring of rice as a result of high gradient of moisture content inside the samples (Yang et al, 2003). For non-food materials, drying was shown to induce cracking of kaolin samples. Convective drying resulted in cracking at the top of the cylinder samples where the tensile stress are maximum while microwave drying was damaged internally as a result of high pore pressure (Kowalski et al, 2005). Convective drying of kaolin did not result in cracking of the samples but application of combination of convective and microwave led to fracture of the samples (Kowalski and Pawlowski, 2009). Controlled drying can give the desirable bending strength and sintered density of ceramic samples (Misra et al, 2002).

For minimization of energy consumption during drying, several schemes intermittent drying is often practiced (Li et al, 1999; Cnossen et al, 2002; Yang et al, 2003; Kowalski and Pawlowski, 2010[a,b]). Intermittent drying is conducted by supplying different heat inputs during drying time to the materials being dried or exposing the materials to time-varying environment conditions. The intermittent drying was reported to be able to reduce energy consumption significantly while achieving the similar moisture content (Chou at al., 2000; Chua et al., 2001). Saving of effective drying time of 25%, 48% and 61% was revealed by intermittent drying with fractions of heating time to total drying time of 0.25, 0.5 and 0.67 (Chou et al., 2000). In addition, infrared-heating drying, microwave drying and ultrasonic-assisted drying have been implemented and it was reported to result in accelerated drying rate (Jain and Pathare, 2004; Sharma et al, 2005; Allanic et al, 2009; Jambrak et al, 2007; Garcia-Perez et al, 2007; 2009; Aversa et al, 2011). Application of infrared-heating with intensity of 2.3 $kW.m^{-2}$ and maintaining the similar operating conditions of drying of polymer solution was shown to increase the drying rate to more than double that of convective drying (Allanic et al, 2006). The application of infrared heating-drying of blueberries was reported to make the drying rate of blueberries three times higher than that of convective drying with the drying air temperature of $60^{\circ}C$ (Shi et al, 2008). Similarly, the microwave drying was reported to

result in much higher drying rate than the conventional one so that significant reduction of the drying time can be achieved (Prabhanjan et al, 1995; Wang and Chen, 2000; Alibas, 2007). In addition, the application of ultrasonic-assisted drying was indicated to result in higher drying rate than the conventional convective drying (Ortuno et al, 2010; Jambrak et al, 2007; Garcia-Perez et al, 2007; 2009; Aversa et al, 2011). It was reported that the ultrasonic-assisted drying alters the mass transfer properties while require less power input than hot air drying (Ortuno et al, 2010). Similarly, the increase of power of ultrasound increases the diffusivity of materials being dried (Garcia-Perez et al, 2007).

The intermittent drying, infrared-heating drying, microwave drying and were also found to yield better product quality than the conventional convective drying (Prabhanjan et al, 1995; Li et al, 1999; Cnossen et al, 2002; Yang et al, 2003; Mulet et al, 2003; Sumnu et al, 2005; Alibas et al, 2007; Kowalski and Pawlowski, 2010[a,b]). For intermittent drying, tempering was shown to affect significantly the internal moisture redistribution, which is favorable to prevent fissuring of rice (Li et al., 1999; Cnossen et al., 2002). The reduction of non-enzymatic browning and loss of ascorbic acid and beta carotene can be achieved by the intermittent drying (Chou et al., 2000; Thomkapanich et al., 2007). For non-food materials, the application of intermittent drying resulted in minimized cracks (Kowalski and Pawlowski, 2010[a,b]). The combination application of hot air and microwave drying was shown to give better surface color and lower rehydration ratio of the food products than the conventional hot air drying (Sumnu et al, 2005; Alibas, 2007; Orsat et al, 2007). The application of infrared-heating drying was also shown to give better texture, firmer, and more cohesive than the conventional drying (Nsonzi & Ramaswamy; 1998; Fernandes et al, 2006; Shi et al, 2008). Similarly, ultrasonic-assisted drying was shown to be able to preserve the qualities of color, flavor and nutrition during drying (Mulet et al, 2003).

Another possible method of process intensification of drying is ultrasonic-assisted drying. This drying method has been implemented to various ranges of materials including vegetables, sugar crystals, powdered milk, coal, polymer and sludge (Fairbanks, 1984; Boistier-Marquis et al, 1999; Gallego-Juarez et al, 1998). The application of ultrasound-assisted drying was indicated to result in higher drying rate than the conventional convective drying (Ortuno et al, 2010; Jambrak et al, 2007; Garcia-Perez et al, 2007; 2009; Aversa et al, 2011). It was reported that the ultrasonic-assisted drying alters the mass transfer properties

while require less power input than hot air drying (Ortuno et al, 2010). The increase of the power intensity of ultrasound above the threshold value results in an increase of drying rate (Garcia-Perez et al, 2006). Similarly, the increase of power of ultrasound increases the diffusivity of materials being dried (Garcia-Perez et al, 2007). Ultrasound may induce contraction and refraction of materials being dried; during contraction small amount of water may be expelled towards the surface (Gallego-Juarez, 2006). In addition, ultrasound drying was shown to be able to preserve the qualities of color, flavor and nutrition during drying (Mulet et al, 2003).

Drying model is useful for assisting in process design and maintaining product quality during drying. The useful model is the one which can capture the physics of drying process, require minimum sets of experiments to generate the parameters and offer simplicity in mathematical modeling and solution. For ultrasonic-assisted drying, several models have been implemented to describe the process (Garcia-Perez et al, 2007; 2009; 2011; Ortuno et al, 2010; Schossler et al, 2012). Most of the modeling implemented diffusion-based model to model the ultrasonic-assisted drying Garcia-Perez et al, 2007; 2009; 2011; Ortuno et al, 2010; Schossler et al, 2012). Crank-diffusion-based model was implemented by several researchers (Garcia-Perez et al, 2007; 2009; 2011; Schossler et al, 2012). However, this model is valid only for isothermal, negligible shrinkage and negligible external resistance (Crank, 1975; Seth and Sarkar, 2004; Doymaz, 2008; Vega-Galvez et al, 2008). The effective-diffusion model was applied by Ortuno et al (2010) and Garcia-Perez et al (2011). The model was shown to model the ultrasonic-assisted drying reasonably well but the model requires several sets of experiments followed by non-linear optimization to generate the diffusivity function (Ortuno et al, 2010; Garcia-Perez et al, 2011).

The reaction engineering approach (REA) is simple drying model proposed by X.D. Chen in 1996 and implemented in various drying systems. The REA takes advantages of simplicity, minimum number of experiments to generate the parameters and accuracy (Chen and Xie, 1997; Chen, 2008). The reaction engineering approach (REA) was applied to describe convective drying of thin layer of food materials and it was proven to be accurate and robust (Chen, Pirini, Ozilgen, 2001; Chen and Lin, 2005). The application of the REA has also been shown to be useful for non-food materials (Putranto, Chen and Webley, 2010[a,b]). Indeed, the REA has been proven to be able to model the cyclic drying of food materials and

non-food materials well (Putranto, Chen and Webley, 2010[b], Putranto, Xiao, Chen and Webley, 2011). The REA has also been revealed to be accurate to model the heat treatment of wood which is essentially a drying process under linearly-increased gas temperature (Putranto, Chen, Xiao, Webley, 2011). Similarly, the REA was also shown to be accurate to describe the intermittent drying of kaolin under slow periodically changed drying air temperature and humidity (Putranto, Chen, Devahastin, Xiao and Webley, 2011). Similarly, the REA has been shown to describe baking and roasting very well (Putranto, Chen and Zhou, 2011; Putranto and Chen, 2012[a]).

Due to the complex phenomena of ultrasonic-assisted drying and intermittent drying, it is worthwhile to implement the REA to describe the process and apply the model to evaluate the mechanisms of the processes. Although the REA has been shown to model several challenging drying cases very well, it may be a challenge for the REA to model ultrasonic-assisted and intermittent drying since the processes are relatively complex. This study is aimed to investigate and assess the applicability of the REA to model the ultrasonic-assisted drying as well as use the REA to study the mechanisms of ultrasonic-assisted drying. The outline of the paper is as follows: the REA is briefly introduced followed by the brief review of the experimental details. The results of modeling and the mechanisms of ultrasonic-assisted drying are discussed subsequently.

1.2 Research objectives

Because of the efficiency of the REA so far, it is worthwhile to develop the REA framework and investigate its applicability to model the ultrasonic-assisted and intermittent drying. The main objectives of this study are to develop the REA framework in an innovative manner, apply and evaluate its accuracy to describe various challenging drying processes. The REA framework is also developed more comprehensively in order to obtain better understanding of transport phenomena of drying process. The main objectives are divided into several specific objectives including:

1. To develop, implement and evaluate the accuracy of the lumped reaction engineering approach (L-REA) to describe the ultrasonic-assisted drying.

2. To develop, apply and evaluate the accuracy of the spatial reaction engineering approach (S-REA) as non-equilibrium multiphase drying approach to model the intermittent drying.

1.3 Scope of research

This research is focused on the development and assessment of accuracy of the reaction engineering approach (REA) framework to model various challenging drying processes. The L-REA (lumped reaction engineering approach) is developed and implemented to describe ultrasonic-assisted drying. The validity of the L-REA to model the above cases is tested against published experimental data and the accuracy is then evaluated.

By using the REA as local evaporation rate, the S-REA (spatial reaction engineering approach) is developed as non-equilibrium multiphase drying model and applied to model the intermittent drying The validity of the REA to model the local evaporation rate as well as the accuracy of S-REA to model these cases are tested against published experimental data. The accuracy is then assessed.

1.4 Expected outcomes

It is expected that this research project has the outcomes of publications in:

1. 1 international refereed journal (Drying Technology or Journal of Food Engineering or Chemical Engineering and Processing: Process Intensification)
2. 1 national conference paper

The expected outcomes are reasonable considering the originality and depth of the research and the experience of the main researcher (Aditya Putranto) in publications in the area of drying technology (See Appendix: Published international peer-reviewed journals and conference papers from Aditya Putranto)

1.5 Expected outputs

It is expected that this research has output of effective mathematical model which can be used for process design and product quality purposes. For process design, the model can be applied to design a new brand dryer and evaluation of performance of existing dryer. The model can be implemented to evaluate the energy consumption as well as the profiles of moisture content and temperature inside the dryer so that troubleshooting and optimization can be conducted. For product quality purpose, the profiles of moisture content and temperature generated by the model can be used to indicate the quality level of the products being dried.

CHAPTER 2

LITERATURE REVIEW

In this chapter, various mathematical models proposed and implemented to describe drying processes are presented. Generally, the mathematical models of drying processes can be classified into: empirical and mechanistic model. The latter one can be further divided into lumped and spatial models. Discussions of these models are given below.

2.1 Empirical models

Several empirical models were applied to model thin layer drying including Page, Newton, Modified Page, Henderson Pabis, logarithmic, two term, two term exponential, Midili and Verma (Page; 1949; Westerman, White and Ross, 1973; Overhults et al, 1973; Henderson, 1974; Wang and Singh, 1978; Sharaf-Eldeen et al, 1980; Bengtsson et al, 1998; Yagcioglu et al, 1999; Midilli et al, 2002). It is revealed that the empirical models describe the drying rate reasonably well but the models are not physically meaningful because of incapable of capturing physics during drying. In addition, the models are not valid for other conditions being tested. This makes the application of the models very limited. Further investigation indicates that the empirical model is also incapable of describing drying kinetics under time-varying ambient conditions (Baini and Langrish, 2007). Several empirical drying models are shown in **Table 2.1**.

Table 2.1 Empirical models of drying kinetics

No.	Model name	Model	Equation no.
1.	Newton	$MR = \exp(-kt)$	(2.1-1)
2.	Page	$MR = \exp(-kt^n)$	(2.1-2)
3.	Modified Page	$MR = \exp[-(kt)^n]$	(2.1-3)
4.	Henderson Pabis	$MR = a\exp(-kt)$	(2.1-4)
5.	Logarithmic	$MR = a\exp(-kt) + c$	(2.1-5)
6.	Two term	$MR = a\exp(-k_0 t) + b\exp(-k_1 t)$	(2.1-6)
7.	Two term exponential	$MR = a\exp(-kt) + (1-a)\exp(-kat)$	(2.1-7)
8.	Midili et al	$MR = a\exp(-kt^n) + bt$	(2.1-8)
9.	Verma	$MR = a\exp(-kt) + (1-a)\exp(-gt)$	(2.1-9)

where MR is the moisture ratio, t is time (s), k, n, a, b, c, g, k_0 and k_1 are model constants.

2.2 Lumped models

Two models using lumped models to describe drying kinetics are characteristics drying rate curve (CDRC) (Keey, 1978; 1992; Langrish and Kockel, 2001) and reaction engineering approach (REA) (Chen and Chen, 1997; Chen and Xie, 1997; Chen, 2008).

2.1 Characteristics drying rate curve (CDRC)

In CDRC, the drying rate is modeled as (Keey, 1978; 1992) as:

$$N = \zeta N_c \tag{2.2-1}$$

where $X>X_c$, $\zeta=1$ and for $X<X_c$, $\zeta=f(\Phi)$,

where N is the flux of drying rate (kg $H_2O.m^{-2}.s^{-1}$), N_c is the drying rate at critical condition (kg $H_2O.m^{-2}.s^{-1}$), ζ is the coefficient representing the relative drying rate, Φ is the characteristics moisture content, X is moisture content on dry basis (kg H_2O.kg dry $solids^{-1}$) and X_c is the critical moisture content on dry basis (kg H_2O.kg dry $solids^{-1}$).

The drying rate at critical conditions is expressed as:

$$N_c = h_m(\rho_{v,sat}(T_{wb}) - \rho_{v,b}) \tag{2.2-2}$$

where h_m is the mass transfer coefficient ($m.s^{-1}$), T_{wb} is the wet bulb temperature (K), $\rho_{v,sat}$ is the saturated water vapor concentration ($kg.m^{-3}$) and $\rho_{v,b}$ is the water vapor concentration of drying medium ($kg.m^{-3}$).

The relative drying rate can be related to the moisture content by:

$$\zeta = \Phi^j \tag{2.2-3}$$

where j is the coefficient representing sensitivity of the relative drying rate towards the characteristics moisture content.

The characteristics moisture content is written as:

$$\Phi = \frac{X - X_e}{X_c - X_e} \tag{2.2-4}$$

where X_e is the equilibrium moisture content (kg H_2O.kg dry $solids^{-1}$).

Combining equation (2.2-3) and (2.2-4) results in:

$$\zeta = \left(\frac{X - X_e}{X_c - X_e}\right)^j \tag{2.2-5}$$

In order to obtain the profile of moisture content and temperature of materials being dried, the mass balance applying CDRC needs be coupled with the heat balance (Langrish and Kockel, 2001). CDRC was applied to model drying kinetics of milk droplet and reasonable agreement

with experimental data was observed (Langrish and Kockel, 2001). However, the CDRC model was shown not to be able to model the intermittent drying (Baini and Langrish, 2007).

2.2. Reaction engineering approach (REA)

The general REA is an application of chemical reaction engineering principles to model drying kinetics which was first reported in 1997 (Chen, 2008). In this approach, evaporation is modeled as zero-order kinetics with activation energy while condensation is described as first order wetting reaction with respect to drying air solvent vapor concentration without activation energy (Chen, 2008). The REA approach offers the advantage of being expressed in terms of simple ordinary differential equation with respect to time. This negates the complications arising from use of partial differential equation (Chen and Xie, 1997). This approach has been firstly employed to express the overall drying rate for the entire object being dried – a lumped approach. A summary of the developments of the lumped approach of REA was, given by Chen (2008).

Generally, with no assumption, the drying rate of a material can be expressed as:

$$m_s \frac{dX}{dt} = -h_m A(\rho_{v,s} - \rho_{v,b}) \qquad (2.2\text{-}6)$$

where m_s is the dried mass of thin layer material (kg), X is the average moisture content on dry basis ($kg.kg^{-1}$), t is time (s), $\rho_{v,s}$ is the water vapor concentration at interface ($kg.m^{-3}$), $\rho_{v,b}$ is the water vapor concentration in the drying medium ($kg.m^{-3}$), h_m is the mass transfer coefficient ($m.s^{-1}$) and A is surface area of the material (m^2).

Equation (2.2-6) is a basic mass transfer equation. The convective mass transfer coefficient (h_m) is determined based on the established Sherwood number correlations for the geometry and flow condition of concern or can be established experimentally for the specific drying conditions involved (Lin and Chen, 2002; Kar and Chen, 2009). The surface vapor concentration ($\rho_{v,s}$) can then be scaled against saturated vapor concentration ($\rho_{v,sat}$) using the following equation (Chen and Chen, 1997; Chen and Xie, 1997; Chen, 2008):

$$\rho_{v,s} = \exp\left(\frac{-\Delta E_v}{RT_s}\right)\rho_{v,sat}(T_s) \tag{2.2-7}$$

where ΔE_v represents the additional difficulty to remove moisture from the material beyond the free water effect. This ΔE_v is the average moisture content (X) dependent. T_s is the surface temperature of the material being dried (K) and $\rho_{v,sat}$ for water vapor can still be estimated by:

$$\rho_{v,sat} = 4.844\times10^{-9}(T_s - 273)^4 - 1.4807\times10^{-7}(T_s - 273)^3 + 2.6572\times10^{-5}(T_s - 273)^2 - 4.8613\times10^{-5}(T_s - 273) + 8.342\times10^{-3} \tag{2.2-8}$$

based on the data summarized by Keey (1992).

When material is 'thermally' thin, the surface temperature is considered to be the same as the sample temperature (Chen and Peng, 2005; Patel and Chen, 2008), i.e. $T_s \approx T$.

The mass balance (equation 2.2-6) is then neatly expressed as:

$$m_s \frac{dX}{dt} = -h_m A\left[\exp(\frac{-\Delta E_v}{RT})\rho_{v,sat}(T) - \rho_{v,b}\right] \tag{2.2-9}$$

From equation (2.1-4), it can be observed that the REA is expressed in the first order ordinary differential equation with respect to time and the model is the core of the lumped reaction engineering approach, i.e. the L-REA. It must be noted that, though the average moisture content is used, the L-REA does not assume uniform moisture content. Of course, no spatial distribution of moisture content can be computed using L-REA. The L-REA may also be applied to cases where the temperature within the material is not uniform as long as the surface temperature can be determined or predicted accurately.

The activation energy (ΔE_v) (which is the characteristic of the material being dried; it is material dependent) needs to be determined experimentally. Upon the attainment of the drying data, notably the surface temperature of the material (or the sample temperature in the case of thermally thin situation) and moisture loss against time, plus the information about the external mass transfer coefficient, one can obtain the activation energy. This can be done by re-arranging equation (2.2-9) as follows:

$$\Delta E_v = -RT_s \ln\left[\frac{-m_s \frac{dX}{dt}\frac{1}{h_m A} + \rho_{v,b}}{\rho_{v,sat}(T_s)}\right] \quad (2.2\text{-}10)$$

The rate of moisture loss dX/dt is experimentally determined. The surface area A should also be recorded in drying experiments in the case of shrinkable material. The dependence of activation energy on average moisture content on a dry basis (X) can be normalized as:

$$\frac{\Delta E_v}{\Delta E_{v,b}} = f(X - X_b) \quad (2.2\text{-}11)$$

where f is a function of water content difference, $\Delta E_{v,b}$ is the 'equilibrium' activation energy representing the maximum ΔE_v determined by the relative humidity and temperature of the drying air:

$$\Delta E_{v,b} = -RT_b \ln(RH_b) \quad (2.2\text{-}12)$$

RH_b is the relative humidity of drying air, X_b is the equilibrium moisture content under the condition of the drying air (kg.kg^{-1}) and T_b is the drying air temperature (K).

2.3.Diffusion-based model

The effective diffusion is considered to be a fundamental mechanism of moisture transport in literatures (Pakowski and Adamski, 2007, Mariani et al, 2008; Thuwapanichayanan et al, 2008; Vaquiro et al, 2009). The effective diffusivity is usually used to lump the whole phenomenon during drying including liquid diffusion, vapor diffusion, Darcy's flow, capillary flow and evaporation/condensation (Pakowski and Adamski, 2007, Mariani et al, 2008; Thuwapanichayanan et al, 2008; Vaquiro et al, 2009). For one-dimensional of convective drying of a slab, the simplest mathematical model of diffusion of moisture can be expressed as:

$$\frac{\partial C}{\partial t} = \frac{\partial}{\partial x}\left(D\frac{\partial C}{\partial x}\right) \quad (2.3\text{-}1)$$

where C can be considered as concentration of liquid water (kg.m^{-3}), D is the effective diffusivity (m^2.s^{-1}), t is time (s) and x is the axial position (m). Equation (2.3-1) usually does

not consider the shrinkage velocity effect and the most important parameter is the effective diffusivity (*D*).

2.3.1 Crank's effective diffusion

Crank's effective diffusion has been used by several researchers and considered as a fundamental drying model (Crank, 1975; Cihan and Ece, 2001; Hassini et al, 2007; Corzo et al, 2008; Arslan and Ozcan, 2011; Castell-Palou, 2011). However, they usually neglect the criteria of Biot number (*Bi*) and ignore the correct boundary conditions. They often do not report the operating conditions of their experiments in details so that the clear justification of the requirement of the validity of the Crank's effective diffusion cannot be made (Chen, 2007). For slab geometry, the solution of Crank's effective diffusion of equation (2.3-1) can be written as (Crank, 1975):

$$\frac{X - X_e}{X_0 - X_e} = \frac{8}{\pi^2} \sum_{n=0}^{\infty} \frac{1}{(2n+1)^2} \exp[-(2n+1)^2 \frac{\pi^2}{L^2} D_{eff,l} t] \qquad (2.3\text{-}2)$$

where D is the effective diffusivity ($m^2.s^{-1}$), X is the moisture content on dry basis (kg water.kg dry $solids^{-1}$) which can be evaluated by ($X=C/\rho_s$), X_0 is the initial moisture content (kg water.kg dry $solids^{-1}$), X_e is the equilibrium moisture content (kg water.kg dry $solids^{-1}$) and L is the half thickness (m) where $L=0.5b$ and the materials are dried symmetrically. For long time period of drying, only the first term of equation (2.3-2) is significant so that equation (2.3-2) can be simplified into (Crank, 1975):

$$\ln(\frac{X - X_e}{X_0 - X_e}) \approx \ln(\frac{8}{\pi^2}) - (\frac{\pi^2}{4b^2} D_{eff,l}) t \qquad (2.3\text{-}3)$$

The Crank's effective diffusion should only be valid for the conditions of isothermal drying, negligible shrinkage, negligible external resistance, constant diffusivity and uniform initial moisture content (Crank, 1975). In addition, the approach should only correlate well with the experimental data for towards the end of drying (Srikatden and Roberts, 2006). However, this has been implemented largely where the assumptions may not be fulfilled and justifications are not made (Cihan and Ece, 2001; Hassini et al, 2007; Corzo et al, 2008; Arslan and Ozcan, 2011; Castell-Palou, 2011)

In addition, the Crank's effective diffusion is based on the surface boundary conditions (at $x=L$, for the slab geometry) of (Crank, 1975):

$$-D_{eff,l}\frac{dX}{dx}=\beta(X_s-X_e) \tag{2.3-4}$$

where D_{eff} is the effective liquid water diffusivity ($m^2.s^{-1}$), X_s is the surface moisture content (kg water.kg dry $solids^{-1}$).

Equation (2.3-4) is in contrast of the boundary conditions of vapor transfer which can be expressed as (Chen, 2007):

$$-D_v\frac{dC_v}{dx}=\beta(\rho_{v,s}-\rho_{v,e}) \tag{2.3-5}$$

where D_v is the effective vapor diffusivity ($m^2.s^{-1}$), C_v is the concentration of water vapor ($kg.m^{-3}$), $\rho_{v,s}$ is the surface water vapor concentration ($kg.m^{-3}$) and $\rho_{v,e}$ is the equilibrium water vapor concentration ($kg.m^{-3}$) which should be similar to the ambient water vapor concentration.

Equations (2.3-4) and (2.3-5) are similar if only at the interface, the moisture content is in equilibrium with the water vapor concentration (Chen, 2007).

2.3.2 Several formulations of diffusion-based models

Various formulations of diffusion-based models have been implemented extensively by a lot of researchers (Cihan and Ece, 2001; Adhikari et al, 2004; Corzo et al, 2008; Vaquiro et al, 2009; Kar and Chen, 2009). The diffusion-based models are usually implemented as the mass balance coupled with the heat balance (Adhikari et al, 2004; Pakowski and Adamski, 2007; Guine, 2008; Kar and Chen, 2009; Vaquiro et al, 2009). However, several researchers (Viollaz and Rovedo, 2002; Loulou et al, 2006; Batista et al, 2007; Garcia-Perez et al, 2009) implemented the diffusion-based model without coupling with the heat balance.

Vaquiro et al (2009) used the diffusion-based model implementing the effective diffusivity coupled with the heat balance to describe the drying kinetics of a cube of mango tissues dried uniformly in *x*, *y* and *z* directions (Sanjuan et al, 2004). By implementing the

diffusion-based model, the mass balance of convective drying of mango tissues can be expressed as (Vaquiro et al, 2009):

$$\frac{\partial}{\partial x}\left(D_e \frac{\partial X}{\partial x}\right)+\frac{\partial}{\partial y}\left(D_e \frac{\partial X}{\partial y}\right)+\frac{\partial}{\partial z}\left(D_e \frac{\partial X}{\partial z}\right)=\frac{\partial X}{\partial t} \tag{2.3-6}$$

with the initial and boundary conditions:

$$t=0,\ X = X_0 \tag{2.3-7}$$

$$x=0, y=0, z=0,\ \frac{\partial X}{\partial x}=\frac{\partial X}{\partial y}=\frac{\partial X}{\partial z}=0 \tag{2.3-8}$$

$$x=L, D_e\rho_s \frac{\partial X}{\partial x}(L,y,z,t) = -h_m \frac{M_w}{R}[\frac{\varphi(L,y,z,t)P_s(L,y,z,t)}{T(L,y,z,t)} - \frac{\varphi_\infty P_{s_\infty}}{T_\infty}] \tag{2.3-9}$$

$$y=L,\ D_e\rho_s \frac{\partial X}{\partial x}(x,L,z,t) = -h_m \frac{M_w}{R}[\frac{\varphi(x,L,z,t)P_s(x,L,z,t)}{T(x,L,z,t)} - \frac{\varphi_\infty P_{s_\infty}}{T_\infty}] \tag{2.3-10}$$

$$z=L,\ D_e\rho_s \frac{\partial X}{\partial x}(x,y,L,t) = -h_m \frac{M_w}{R}[\frac{\varphi(x,y,L,t)P_s(x,y,L,t)}{T(x,y,L,t)} - \frac{\varphi_\infty P_{s_\infty}}{T_\infty}] \tag{2.3-11}$$

where D_e is the effective diffusivity (m^2s^{-1}), ρ_s is the density of solid ($kg.m^{-3}$), X is the moisture content on dry basis (kg $H_2O.m^{-3}$), h_m is the mass transfer coefficient ($m.s^{-1}$), M_w is the molecular weight of water ($kg.kmol^{-1}$), φ is the surface relative humidity, P_s is the saturated vapor pressure (Pa), T is sample temperature (K), φ_∞ is the drying air relative humidity, $P_{s\infty}$ is the vapor pressure in drying air (Pa), T_∞ is the drying air temperature., L is the thickness of sample (m).

while the heat balance can be expressed as (Vaquiro et al, 2009):

$$\begin{aligned}&\frac{\partial}{\partial x}\left(k\frac{\partial T}{\partial x}\right)+\frac{\partial}{\partial y}\left(k\frac{\partial T}{\partial y}\right)+\frac{\partial}{\partial z}\left(k\frac{\partial T}{\partial z}\right)= \\ &\rho_{ds}(C_{p_{ds}}+XC_{p_w})\frac{\partial T}{\partial t}-D_e\rho_{ds}C_{p_w}\left(\frac{\partial X}{\partial x}\frac{\partial T}{\partial x}+\frac{\partial X}{\partial y}\frac{\partial T}{\partial y}+\frac{\partial X}{\partial z}\frac{\partial T}{\partial z}\right)\end{aligned} \tag{2.3-12}$$

with the initial and boundary conditions:

$$t=0,\ T = T_0 \tag{2.3-13}$$

$$x=0,\ y=0,\ z=0,\ \frac{\partial T}{\partial x} = \frac{\partial T}{\partial y} = \frac{\partial T}{\partial z} = 0 \tag{2.3-14}$$

$$x=L,\ -k\frac{\partial T}{\partial x}(L,y,z,t) = h[T(L,y,z,t) - T_\infty] - D_e\rho_{ds}\frac{\partial X}{\partial x}(L,y,z,t)Q_s \tag{2.3-15}$$

$$y=L,\ -k\frac{\partial T}{\partial y}(x,L,z,t) = h[T(x,L,z,t) - T_\infty] - D_e\rho_{ds}\frac{\partial X}{\partial y}(x,L,z,t)Q_s \tag{2.3-16}$$

$$z=L,\ -k\frac{\partial T}{\partial z}(x,y,L,t) = h[T(x,y,L,t) - T_\infty] - D_e\rho_{ds}\frac{\partial X}{\partial z}(x,L,z,t)Q_s \tag{2.3-17}$$

where k is the thermal conductivity of sample ($W.m^{-1}.K^{-1}$), h is the heat transfer coefficient ($W.m^{-2}.K^{-1}$), ρ_{ds} is the density of dry solid ($kg.m^{-3}$), Q_s is the heat of evaporation of water ($J.kg^{-1}$), Cp_{ds} is the specific heat of dry solid ($J.kg^{-1}.K^{-1}$), Cp_w is the specific heat of water ($J.kg^{-1}.K^{-1}$).

Several sets of experiments followed by optimization procedures were carried out in order to establish the effective diffusivity as function of temperature and moisture content. Vaquiro et al (2009) reported that the effective diffusivity of mango tissues can be represented as:

$$D_e = 2.933\times10^{-3}\exp[\frac{-38924}{8.314T}(\frac{X}{X+1})^{-1.885\times10^{-2}}] \tag{2.3-18}$$

By using the diffusion-based model shown in equation (2.3-6) with the initial and boundary conditions indicated in equations (2.3-7) to (2.3-11) in conjunction with the heat balance shown in equation (2.3-12) in conjunction with the initial and boundary conditions represented in equations (2.3-13) to (2.3-17), a reasonable agreement towards the experimental data was shown (Vaquiro et al, 2009).

CHAPTER 3

METHODOLOGY

3.1. Ultrasonic-assisted drying

The meaningful experimental data for study of ultrasound-assisted drying is derived from the previous published work of Garcia-Perez et al (2009). For better understanding of the modeling implemented here, the experimental details of Garcia-Perez et al (2009) are reviewed briefly here. The experimental setup is shown in Figure 3.1. The raw materials of lemon were obtained from Javea, Spain in the end stage of ripeness. The lemon-peel was separated from the pulp by hand and the samples of lemon-peel were cut into slabs with thickness of 7 mm (Garcia-Perez et al, 2009). The convective dryer equipped by the ultrasound power generator was used to study the drying kinetics of lemon-peel. The details of the equipment were presented previously (Garcia-Perez et al, 2006). The ultrasonic generator produced a high intensity ultrasonic field and reached an average sound pressure level of 154.3 dB. The digital power meter was used to monitor the voltage, intensity, power, phase and frequency of the electric signal (Garcia-Perez et al, 2009). Convective drying experiments were conducted at drying air temperature of 40 °C and air velocity of 1 $m.s^{-1}$. The ultrasonic-assisted drying of lemon-peel is conducted at various levels of ultrasonic power i.e. 8, 12, 21, 29 and 37 kW/m^3. This was conducted by adjusting several electric powers to the ultrasonic transducer. The load density of lemon-peel of 36 $kg.m^{-3}$ was used for the experiments. During drying, the air velocity and temperature were controlled by a PID controller and the weight of the samples was monitored by a balance wired to the sample load chamber (Garcia-Perez et al, 2009).

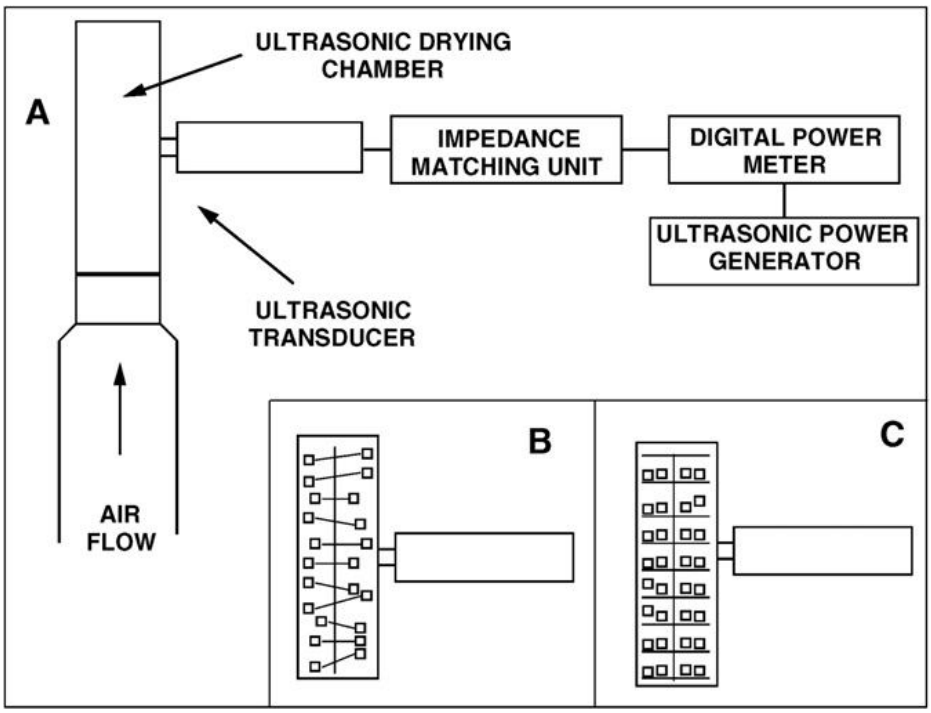

Figure 3.1. Equipment setup for ultrasonic-assisted drying (Garcia-Perez et al, 2006)

3.2. Lumped reaction engineering approach (L-REA) model for ultrasonic-assisted drying

The reaction engineering approach (REA) is an application of a chemical reactor engineering principle to model drying kinetics first proposed by X.D. Chen in 1996 (Chen and Xie, 1997; Chen, 2008). A recent summary of the reaction engineering approach (REA) was given by Chen (2008).

In general, the drying rate of a material can be expressed as:

$$m_s \frac{dX}{dt} = -h_m A\left(\rho_{v,s} - \rho_{v,b}\right) \qquad (3.2\text{-}1)$$

where m_s is the dried mass of material (kg), t is time (s), X is the average moisture content on a dry basis (kg.kg^{-1}), $\rho_{v,s}$ is the vapor concentration at the material-air interface (kg.m^{-3}), $\rho_{v,b}$ is the vapor concentration in the drying medium (kg.m^{-3}), h_m is the mass transfer coefficient (m.s^{-1}) and A is the surface area of the material (m^2). Equation (1) does not involve much

assumption at all. The mass transfer coefficient (h_m) is determined based on the established Sherwood number correlations for the geometry and flow condition of concern. The mass transfer coefficient (h_m) may also be established experimentally and directly for the specific drying conditions involved. The surface vapor concentration ($\rho_{v,s}$) can be scaled against saturated vapor concentration ($\rho_{v,sat}$) using the following equation (Chen and Xie, 1997; Chen, 2008):

$$\rho_{v,s} = \exp\left(\frac{-\Delta E_v}{RT}\right)\rho_{v,sat}(T) \tag{3.2-2}$$

where the term $\exp\left(\frac{-\Delta E_v}{RT}\right)$ represents the relative humidity at the surface of the solid domain exposed to the gas phase. ΔE_v represents the additional difficulty to remove moisture from the material beyond the free water effect. This ΔE_v is moisture content (X) dependent. T is the temperature of the material being dried (K) and $\rho_{v,sat}$ (kg.m^{-3}) for water can be estimated with the following correlation:

$$\rho_{v,sat} = 4.844\times10^{-9}(T-273)^4 - 1.4807\times10^{-7}(T-273)^3 + 2.6572\times10^{-5}(T-273)^2 - 4.8613\times10^{-5}(T-273) + 8.342\times10^{-3} \tag{3.2-3}$$

where T is temperature (K) based on the data summarized by Keey (1992).

The mass balance (equation 1)can then be rewritten:

$$m_s\frac{dX}{dt} = -h_m A\left[\exp(\frac{-\Delta E_v}{RT})\rho_{v,sat} - \rho_{v,b}\right] \tag{3.2-4}$$

Equation (3.2-4) is an ordinary differential equation with respect to time predicting the change of moisture content during drying. The model shown in equation (3.2-4) is called the lumped reaction engineering approach (L-REA).

The activation energy (ΔE_v) is determined experimentally by rearranging equation (3.2-4) in the following:

$$\Delta E_v = -RT \ln\left[\frac{-m_s \frac{dX}{dt}\frac{1}{h_m A} + \rho_{v,b}}{\rho_{v,sat}}\right] \tag{3.2-5}$$

where *dX/dt* is the rate of mean water content change during drying determined experimentally. Basically, for a given drying run, the parameters on the RHS (right hand side) are all known so that the activation energy can be obtained. The dependence of activation energy on moisture content *X* can be normalized as:

$$\frac{\Delta E_v}{\Delta E_{v,b}} = f\left(X - X_b\right) \tag{3.2-6}$$

where *f* is a function of water content difference, $\Delta E_{v,b}$ is the 'equilibrium' activation energy which is the maximum ΔE_v under the relative humidity and at the temperature of the drying air:

$$\Delta E_{v,b} = -RT_b \ln\left(RH_b\right) \tag{3.2-7}$$

X_b is the equilibrium moisture content on a dry basis corresponding to RH_b (relative humidity of drying air) and T_b (drying air temperature) which can be related to one another through the equilibrium isotherm of the same material.

For similar drying condition and initial water content, it is possible to obtain the necessary REA parameters (apart from the equilibrium isotherm), expressed in the relative activation energy ($\Delta E_v/\Delta E_{v,b}$) as indicated in equation (3.2-6), in one accurate drying experiment. Of course, different temperatures might cause microstructural changes that alter the internal transport characteristics. One cannot rule out running out several experiments to cover the range of practical interest. The relative activation energy ($\Delta E_v/\Delta E_{v,b}$) generated can then be implemented to other drying conditions provided the same material and similar initial moisture content since the relative activation energy usually can collapse to the similar profile (Chen and Xie, 1997; Chen and Lin, 2005; Chen, 2008).

In order to model the convective and ultrasonic-assisted drying of lemon-peel using the reaction engineering approach (REA), the relative activation energy ($\Delta E_v/\Delta E_{v,b}$) is generated from one accurate drying experiment which is the convective drying of lemon-peel

at drying air temperature of 40 °C. The activation energy during drying is evaluated using equation (3.2-5) and divided with the equilibrium activation energy represented in equation (3.2-7) to yield the relative activation energy as mentioned in equation (3.2-6).

The heat balance of convective drying of lemon-peel can be expressed as:

$$\frac{d\left[m_s(1+X)C_pT\right]}{dt} \approx hA(T_b - T) + m_s \frac{dX}{dt}\Delta H_v \qquad (3.2\text{-}8)$$

where m_s is sample mass (kg), C_p is the heat capacity of the sample ($J.kg^{-1}.K^{-1}$), T is the temperature of the sample (K), h is the heat transfer coefficient ($W.m^{-2}.K^{-1}$), ΔH_v is vaporization heat of water ($J.kg^{-1}$), T_b is the gas temperature (K). The drying rate dX/dt is negative when drying occurs.

while the heat balance of the ultrasound-assisted drying of lemon-peel can be written as:

$$\frac{d\left[m_s(1+X)C_pT\right]}{dt} \approx P + hA(T_b - T) + m_s \frac{dX}{dt}\Delta H_v \qquad (3.2\text{-}9)$$

where P is the ultrasonic power received by the sample (W).

In order to yield the profiles of moisture content and temperature during convective drying of lemon-peel, the mass balance implementing the REA shown in equation (3.2-4) is solved simultaneously with the equilibrium activation energy, relative activation energy and heat balance shown in equations (3.2-7), (3.2-8) and (3.2-9) respectively. The ordinary differential solver *ode23s* available in Matlab® (Mathworks Inc, 2012) is used to solve these equations simultaneously. Similarly, for ultrasound-assisted drying, the mass balance implementing the L-REA, equilibrium activation energy and heat balance presented in equations (3.2-4), (3.2-7), (3.2-8) and (3.2-9) are solved simultaneously using *ode23s* available in Matlab® (Mathworks Inc, 2012). The results of the modeling are validated against the experimental data of convective and ultrasonic-assisted drying from the previous published work of Garcia-Perez et al (2009).

In order to model the convective and ultrasonic-assisted drying of lemon-peel using the reaction engineering approach (REA), the relative activation energy ($\Delta E_v/\Delta E_{v,b}$) is generated from one accurate drying experiment which is the convective drying of lemon-peel at drying air temperature of 40 °C. The activation energy during drying is evaluated using equation (5) and divided with the equilibrium activation energy represented in equation (7) to yield the relative activation energy as mentioned in equation (6). The relationship between the relative activation energy and average moisture content can be represented by simple mathematical equation obtained by least square method using Microsoft Excel® (Microsoft Corp, 2011). The relative activation energy can be represented as:

$$\frac{\Delta E_v}{\Delta E_{v,b}} = \left[1 - 0.217(X - X_b)^{0.881}\right]\exp\left[0.163(X - X_b)^{0.322}\right] \quad (8)$$

The good fit of the relative activation energy is shown in Figure 1 (R^2 of 0.998). The format of equation (8) can be varied but in this case equation (8) seems to be sufficient to describe the relative activation energy of drying of lemon-peel.

The heat balance of convective drying of lemon-peel can be expressed as:

$$\frac{d\left[m_s(1+X)C_pT\right]}{dt} \approx hA(T_b - T) + m_s\frac{dX}{dt}\Delta H_v \quad (9)$$

where m_s is sample mass (kg), C_p is the heat capacity of the sample ($J.kg^{-1}.K^{-1}$), T is the temperature of the sample (K), h is the heat transfer coefficient ($W.m^{-2}.K^{-1}$), ΔH_v is vaporization heat of water ($J.kg^{-1}$), T_b is the gas temperature (K). The drying rate dX/dt is negative when drying occurs.

while the heat balance of the ultrasound-assisted drying of lemon-peel can be written as:

$$\frac{d\left[m_s(1+X)C_pT\right]}{dt} \approx P + hA(T_b - T) + m_s\frac{dX}{dt}\Delta H_v \quad (10)$$

where P is the ultrasonic power received by the sample (W).

CHAPTER 4
RESULTS AND DISCUSSION

The profiles of relative activation energy of convective drying are shown in Figure 1. At the beginning of convective drying, the relative activation energy is close to 0 and it increases as drying progresses. When equilibrium moisture content is achieved, the relative activation energy is 1. It increases from 0 at the beginning of drying and approaches to 1 when the equilibrium moisture content is achieved.

For modeling of ultrasound-assisted drying at various intensities in this study, the relative activation energy generated from convective drying run as shown in equation (8) is used. As mentioned before, the good fit between the fitted and experimental activation energy is shown in Figure 1 (R^2 of 0.998).

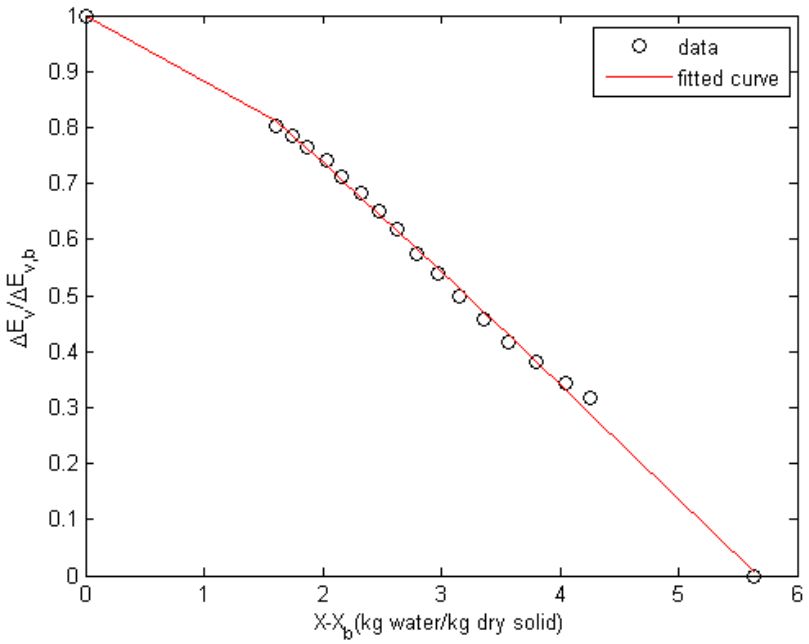

Figure 1. The fitted and experimental relative activation energy ($\Delta E_v/\Delta E_{v,b}$) of convective drying at drying air temperature of 40 °C

Results of modeling using the REA are shown in Figures 2 to 7. Figures 2 and 3 present the results of modeling of convective drying and ultrasonic-assisted drying at intensity of 4 kW.m^{-3} using the REA. A good agreement between the predicted and experimental data is observed. Table 1 indicates that the good agreement is supported by R^2 of higher than 0.995 and *RMSE* lower than 0.086. In addition, the profiles of temperature during drying are shown in Figure 3. Compared to the diffusion-based modeling implemented by Garcia-Perez et al (2009), the REA yields advantages of generating temperature profiles during drying; not shown by the other model.

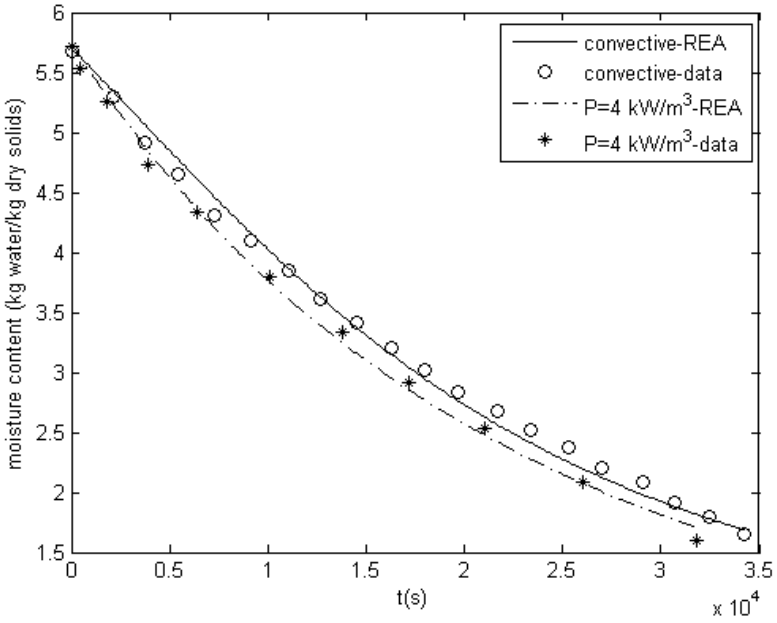

Figure 2. Profiles of moisture content of convective drying at drying air temperature of 40 °C and ultrasonic-assisted drying at intensity of 4 kW.m^{-3}

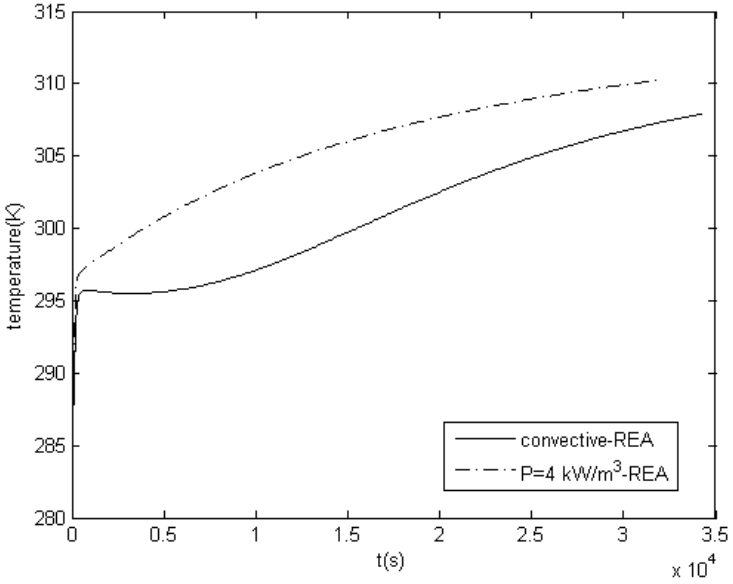

Figure 3. Profiles of temperature of convective drying at drying air temperature of 40 °C and ultrasonic-assisted drying at intensity of 4 kW.m^{-3}

The results of implementation of the REA for ultrasonic-assisted drying at intensity of 8 and 12 kW.m^{-3} are presented in Figures 4 and 5. Figure 4 shows the profiles of moisture content during drying. The REA describes the profiles of moisture content during drying very well. The good agreement is indicated by R^2 of higher than 0.996 and *RMSE* lower than 0.071 (refer to Table 1). Figure 5 reveals the profiles of temperature during drying. Again, the REA yields the advantages of generating the temperature profiles during drying; not shown by the modeling applied by Garcia-Perez et al (2009). The REA can model the ultrasonic-assisted drying with intensity of 8 and 12 kW.m^{-3} well.

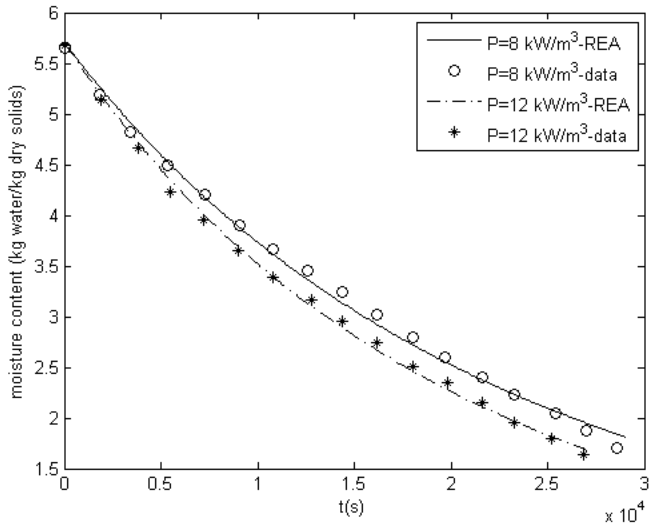

Figure 4. Profiles of moisture content of ultrasonic-assisted drying at intensity of 8 and 12 kW.m^{-3}

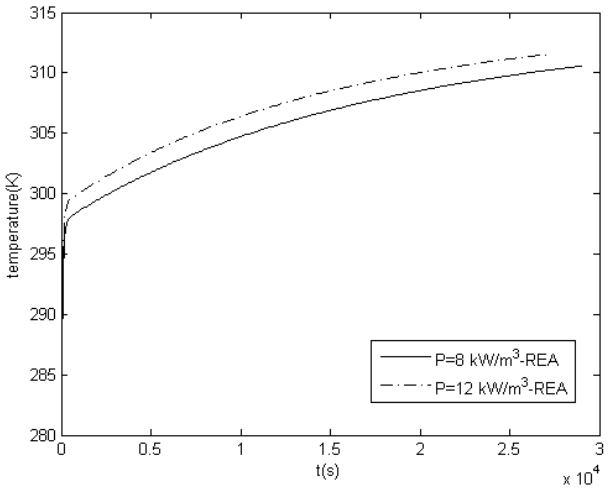

Figure 5. Profiles of temperature of ultrasonic-assisted drying at intensity of 8 and 12 kW.m^{-3}

In addition, the results of modeling of ultrasonic-assisted drying at intensity of 21, 29 and 37 kW.m^{-3} are shown in Figures 6 and 7. The profiles of moisture content during drying are shown in Figure 6. The REA models the profiles of moisture content during ultrasonic-assisted drying at intensity of 21, 29 and 37 kW.m^{-3} very well. The results of modeling match well with the experimental data. The good agreement between the predicted and experimental

data is also confirmed by R^2 and *RMSE* shown in Table 1. Figure 7 presents the profiles of temperature during drying. The REA is indeed accurate to model the ultrasonic-assisted drying at intensity of 21, 29 and 37 kW.m^{-3}.

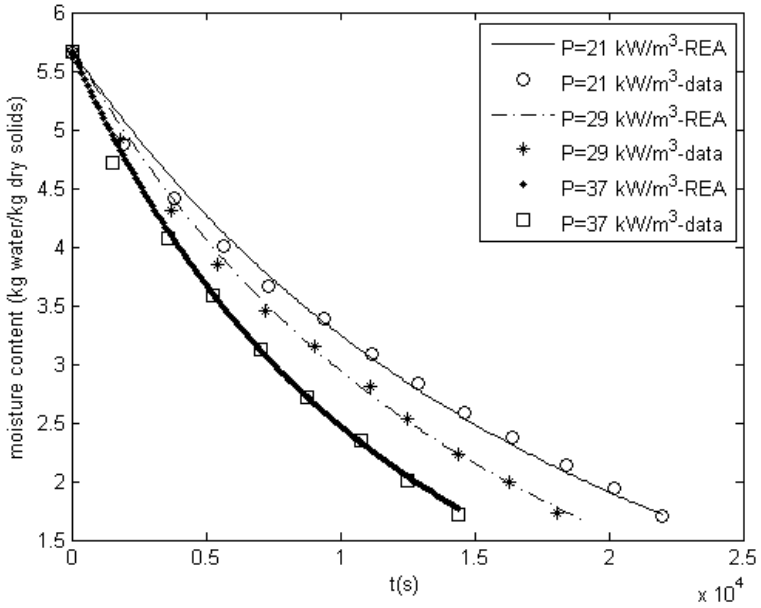

Figure 6. Profiles of moisture content of ultrasonic-assisted drying at intensity of 21, 29 and 37 kW.m^{-3}

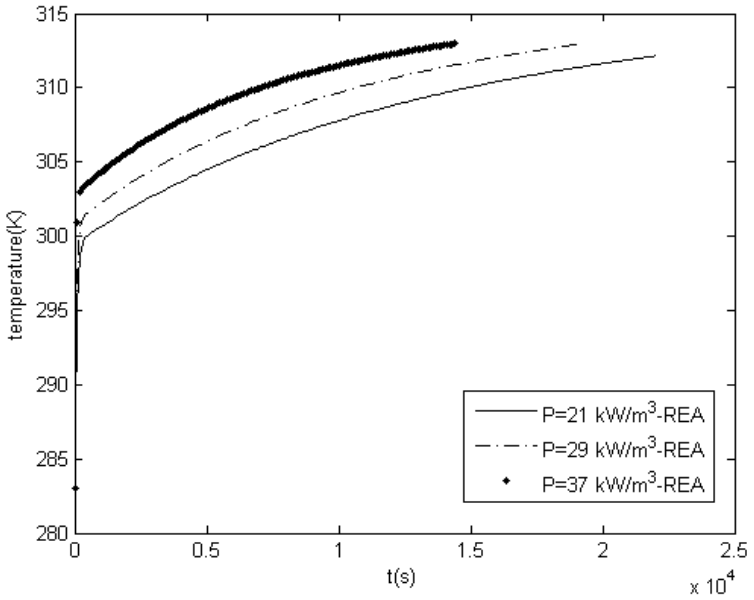

Figure 7. Profiles of temperature of ultrasonic-assisted drying at intensity of 21, 29 and 37 kW.m^{-3}

It has been shown that the REA models the convective and ultrasonic-assisted drying of lemon-peel very well. The relative activation energy generated from one accurate convective drying can be used for modeling of ultrasonic-assisted drying at various intensities. The accuracy of the REA could be because of applicability of the relative activation energy to capture the physics of ultrasonic-assisted drying. Ultrasound wave implemented may alter the internal and external resistance of mass and heat transfer (Scarborough et al, 2006). The ultrasound was postulated to cause "sponge effect" i.e. expansion and compression in the material which facilitates water removal (Garcia-Perez et al, 2007). Application of ultrasonic wave resulted in change of microstructure at the surface and inside the materials. At the surface, the pores were obstructed by wax component scattering (Ortuno et al, 2010) and the ultrasonic wave may result in pressure variation, oscillation and microstreaming which reduces the thickness of boundary layer (Gallego-Juarez et al, 1999). Inside the materials, the ultrasound wave was shown to make the cellular structure were more compressed and destroyed with large air intercellular spaces (Ortuno et al, 2010). It was postulated to cause developed force inside the materials which allows the formation of micro-channel favorable for removal of water vapor (Da Mota and Palau, 1999).

Similarly, the ultrasound wave may promote the growth of new cavities and bubbles inside the materials (de Fuente-Blanco et al, 2006). The applicability of the REA on ultrasonic-assisted drying indicates that the complex mechanisms of ultrasonic-assisted drying can be explained by the relative activation energy. It seems that the relative activation energy can incorporate the alteration of internal and external transfer resulted by ultrasonic wave. The effects of change in microstructure inside the materials and at the surface, expansion-compression inside the materials, oscillation and pressure variation seem to be represented well by the relative activation energy. It can be used to lump all phenomena generated by ultrasonic wave on the materials being dried.

It can be said that the REA is accurate to model the ultrasonic-assisted drying. While the results are accurate, the modeling itself is still simple and requires minimum number of experiments for generate the drying parameters. It can also explain the mechanisms of ultrasonic-assisted drying well. This has extended the application of the REA significantly and revealed that the REA can be used to explain the physics of ultrasound-assisted drying. It has followed the accuracy of the REA to several challenging cases of drying, baking and roasting as well as the ability of the REA to explain the physics of these processes (Putranto et al, 2010[a,b]; Putranto et al, 2010[a-f]; Putranto and Chen, 2012).

Conclusion

In this study, the REA is applied to model the ultrasonic-assisted drying at various intensities. The relative activation energy is generated from one accurate drying experiment is implemented to describe the change of internal behavior inside the materials during ultrasound-assisted drying at various intensities. The results of modeling match well with the experimental data. The REA is accurate to model the ultrasound-assisted drying. The REA can model the ultrasound-assisted drying very well. The mechanisms of ultrasonic-assisted drying can be explained well also by the REA. While the results are accurate, the modeling is still simple. Another significant landmark of the REA on process intensification of drying has been shown here.

References

Allanic, N., Salagnac, P., Glouannec, P., 2006. Convective and radiant drying of a polymer aqueous solution, Heat Mass Transfer 43, 1087-1095.

Aversa, M., Van der Voort, A.J., de Heij, W., Tournois, B., Curcio, S., 2011. An experimental analysis of acoustic drying of carrots: evaluation of heat transfer coefficients in different drying conditions, Drying Technology 29, 239–244.

Boistier-Marquis, E., Lagsir-Oulahal, N., Callard, M., 1999. Applications des ultrasons de puissances en industries alimentaires, Ind. Aliment. Agric. 116, 23–31.

Chen, X.D., 2008. The basics of a REA to modeling air drying of small droplets or thin layer materials, Drying Technol. 26, 627-639.

Chen, X.D., Lin, S.X.Q., 2005. Air drying of milk droplet under constant and time dependent conditions. AIChE J. 51, 1790-1799.

Chen, X.D., Pirini, W., Ozilgen, M., 2001. The REA to modeling drying of thin layer pulped kiwifruit flesh under conditions of small Biot numbers. Chem. Eng. Proc. 40, 311-320.

Chen, X.D., Xie, G.Z., 1997. Fingerprints of the drying behavior of particulate or thin layer food materials established using a reaction engineering model. Trans IChemE, Part C: Food and Bioprod. Proc. 75, 213-222.

Chou, S.K., Chua, K.J., Mujumdar, A.S., Hawlader, M.N.A., Ho,J.C., 2000. On the intermittent drying of an agricultural product, Food Bioprod. Proc. 78, 193-203.

Chua, K.J., Mujumdar, A.S., Hawlader, M.N.A., Chou, S.K., Ho, J.C., 2001. Batch drying of banana pieces - effect of stepwise change in drying air temperature on drying kinetics and product colour, Food Res. Int. 34, 721-731.

Das, I., Das, S.K., Bal, S., 2009. Drying kinetics of high moisture paddy undergoing vibration-assisted infrared (IR) drying, J. Food Eng. 95, 166–171.

Da-Mota, V.M., Palau, E., 1999. Acoustic drying of onion. Drying Technology 17, 855–867.

de la Fuente-Blanco, S., Riera-Franco de Sarabia, E., Acosta- Aparicio, V.M., Blanco-Blanco, A., Gallego-Juarez, J.A. Food drying process by power ultrasound. Ultrasonics 44, 523–527.

Doymaz, I., 2008. Convective drying kinetics of strawberry, Chemical Engineering and Processing 47, 914–919.

Fairbanks, H.V., 1984. Ultrasonically assisted drying of fine particles. Ultrasonics, 260-262.

Gallego-Juarez, J.A., 1998. Some applications of air-borne power ultrasound to food processing, in: M.J.W. Povey, T.J. Mason (Eds.), Ultrasound in Food Processing, Blackie, Glasgow, 127–143.

Gallego-Juarez, J.A., Rodriguez-Corral, G., Galvez-Moraleda, J.C., Yang, T.S., 1999. A new high-intensity ultrasonic technology for food dehydration. Drying Technology 17, 597–608.

Garcia-Perez, J.V., Carcel, J.A, de la Fuente-Blanco, S., de Sarabia, E.R., 2006. Ultrasonic drying of foodstuff in a fluidized bed: Parametric study, Ultrasonics 44, 539-543.

Garcia-Perez, J.V., Carcel, J.A., Benedito, J., Mulet, A., 2007. Power ultrasound mass transfer enhancement in food drying. Food and Bioproducts Processing 85, 247-254.

Garcia-Perez, J.V., Carcel, J.A., Benedito, J., Mulet, A., 2009. Influence of the applied acoustic energy on the drying of carrots and lemon peel, Drying Technology 27, 281–287.

Gunasekaran, S., 1999. Pulsed microwave-vacuum drying of food, Drying Technology 17, 395–412.

Jambrak, A.R., Mason, T.J., Paniwnyk, L., Lelas, V., 2007. Accelerated drying of button mushrooms, Brussels sprouts and cauliflower by applying power ultrasound and its rehydration properties. Journal of Food Engineering 81, 88–97.

Keey, R.B., 1992. Drying of Loose and Particulate Materials, Hemisphere Publishing, New York.

Mathworks Inc., http://www.mathworks.com.au/, accessed on 16 January 2012.

Microsoft Inc., http://office.microsoft.com/en-au/, accessed on 16 January 2012

Mulet, A., Carcel, J.A., Sanjuan, N., Bon, J., 2003. New food drying technologies – use of ultrasound, Food Science and. Technology International 9, 215–221.

Ortuno, C., Perez-Munuera, I., Puig, A., Riera, E., Garcia-Perez, J.V., 2010. Influence of power ultrasound application on mass transport and microstructure of orange peel during hot air drying. Physics Procedia, 153-159.

Pan, Z., Shih, C., McHugh, T.H., Hirschberg, E., 2008. Study of banana dehydration using sequential infrared radiation heating and freeze-drying, LWT - Food Sci. Tech. 41, 1944-1951

Putranto, A., Chen, X.D., 2012. Roasting of barley and coffee modeled using the lumped-reaction engineering approach (L-REA). Drying Technology 30, 475-483.

Putranto, A., Chen, X.D., Webley, P.A., 2010[a], Infrared and convective drying of thin layer of polyvinyl alcohol (PVA)/glycerol/water mixture - The reaction engineering approach (REA). Chemical Engineering and Processing: Process Intensification 49, 348-357.

Putranto, A., Chen, X.D., Webley, P.A., 2010[b], Application of the reaction engineering approach (REA) to model cyclic drying of polyvinyl alcohol(PVA)/glycerol/water mixture. Chemical Engineering Science 65, 5193-5203.

Putranto, A., Chen, X.D., Webley, P.A., 2011[a], Modeling of drying of thick samples of mango and apple tissues using the reaction engineering approach (REA). Drying Technology 29, 961-973.

Putranto, A, Chen, X.D., Xiao, Z., Webley, P.A., 2011[b]. Intermittent drying of mango tissues: implementation of the reaction engineering approach (REA). Industrial Engineering Chemistry Research 50, 1089-1098.

Putranto, A., Chen, X.D., Devahastin, S., Xiao, Z., Webley, P.A., 2011[c]. Application of the reaction engineering approach (REA) to model intermittent drying under time-varying humidity and temperature. Chemical Engineering Science 66, 2149-2156.

Putranto, A., Chen, X.D., Xiao, Z., Webley, P.A., 2011[d]. Mathematical modeling of convective and intermittent drying of rice and coffee using the reaction engineering approach (REA). Journal of Food Engineering 105, 638-646.

Putranto, A., Chen, X.D., Xiao, Z., Webley, P.A., 2011[e]. Modeling of high-temperature treatment of wood by using the reaction engineering approach (REA). Bioresource Technology 102, 6214-6220.

Putranto, A., Chen, X.D., Zhou, W., 2011[f]. Modeling of baking of cake using the reaction engineering approach (REA), Journal of Food Engineering 105, 306-311.

Scarborough, D.E., Sujith, R.I., Zinn, B.T., 2006. The effect of resonant acoustic oscillations on heat and mass transfer rates in a convection air dryer, Drying Technology 24, 931–939.

Schossler, K., Jager, H., Knorr, D., 2012. Effect of continuous and intermittent ultrasound on drying time and effective diffusivity during convective drying of apple and red bell pepper, Journal of Food Engineering 108, 103–110.

Seth, D., Sarkar, A., 2004. A lumped parameter model for effective moisture diffusivity in air drying of foods. Food Bioprod. Process. 82, 183–192

Vega-Galvez, A., Miranda, M., Bilbao-Sainz, B., Uribe, E., Lemus-Mondaca, R., 2008. Empirical modeling of drying process for apple (cv. granny smith) slices at different air temperatures. Journal of Food Process. Preserv. 32, 972–986.